

## Early Stage of Spinodal Decomposition in 2D

S. Joly, A. Raquois, F. Paris, B. Hamdoun, L. Auvray,\* and D. Ausserre†

*Equipe de Physique de l'Etat Condensé (URA CNRS No. 807), Université du Maine, BP 535, 72017 Le Mans Cedex, France*

Y. Gallot

*Institut Charles Sadron, 6 rue Boussingault, 67083 Strasbourg Cedex, France*

(Received 7 March 1996; revised manuscript received 25 June 1996)

A qualitative description of a spinodal decomposition kinetics is proposed. It is made of a linear stage followed by two nonlinear stages, leading, respectively, to higher and lower frequency generation in the spatial order parameter distribution, then followed by the classical Ostwald ripening. This general scheme is supported by a specific experimental study. It concerns the two-dimensional thickness demixion of copolymer thin films made of three to four bilayers. [S0031-9007(96)01677-8]

PACS numbers: 64.75.+g, 61.25.Hq, 68.15.+e

Spinodal decomposition (SD) is usually too fast to be captured in experiments. Also, most of the kinetic investigations are based on scattering techniques which naturally lead to an inspection of the results in the reciprocal Fourier space, where all quantities are integrated over the whole sample. As a consequence, little has been said about local behaviors. On the theoretical side, most of the productive efforts have been concentrated either on extremely short times, where the linear Cahn-Hilliard theory applies, or on last stage kinetics where domains of the two final coexisting phases are stabilized and slowly evolve according to quasistationary principles. Most of the theoretical treatments are also based on a Fourier approach. In this context, the present experimental work is claimed to be original by four aspects: (i) It focuses on the very early stage precisely where our experimental knowledge is so poor [1]. (ii) It gives the direct distribution of the order parameter in space as a function of time [2]. Only the use of a local probe makes it possible. Ours is atomic force microscopy (AFM). (iii) It deals with a nonconventional experimental system for phase transition kinetics in two dimensions that we want to promote as a powerful model system, competitive by many aspects with the more traditional Langmuir monolayers [3]. (iv) It deals with off-critical quenches; the final domain pattern is made of disconnected drops.

The goal of the present Letter is to propose a new qualitative description of the early stage, in which two different nonlinear mechanisms are proposed. The text is organized as follows: The whole kinetics is first exposed in general terms. Our system is then introduced, and experimental results are presented. The connection is finally made with the first part.

The system under consideration belongs to the Ising universality class and satisfies model B constraints [4]. We start from a high temperature homogeneous equilibrium state characterized by a uniform off-critical order parameter  $\Psi_0$ . Operating at constant  $\Psi_0$ , we suddenly quench the system to a temperature  $T$  such that  $(\Psi_0, T)$  is located in the unstable region of the phase diagram. The

spinodal decomposition starts. It will lead, after a long time, to the formation of macroscopic domains characterized by two well defined order parameters  $\Psi_1(T)$  and  $\Psi_2(T)$ . We assume that the majority phase corresponds to  $\Psi_1 < \Psi_2$ .

The kinetics is described as the sketch of successive events illustrated on Fig. 1, which considers a one-dimensional space for the sake of simplicity. The order parameter conservation constraint  $\int d^d \mathbf{r} \times [\Psi(\mathbf{r}) - \Psi_0(\mathbf{r})] = 0$  is a volume conservation condition in the  $(d + 1)$ -dimensional  $\{r, \Psi\}$  space. As a consequence, the time evolution of the spatial distribution of  $\Psi$  can be thought and described in terms of geometric distortions of a hypersurface which limits a closed  $(d + 1)$  volume. For  $d = 1$ , for instance, as on Fig. 1, the arbitrary axis  $\Psi = 0$  and the moving line  $\Psi(x)$  are the two boundaries of a domain with a constant area.

Hence, the first stage right after the quench appears as a roughening of the initially straight line  $\Psi = \Psi_0$ . This stage is classically treated [5] as a linear instability which favors one characteristic wavelength  $\lambda_*$  ( $= \lambda_*^d$  for  $d = 1$ ). In a simplified description conforming to Fig. 1(-a), the roughness spectrum reduces to the dominant mode  $\lambda_*$ . Its amplitude is rapidly increasing with time. The  $\Psi$  line spreads symmetrically towards both  $\Psi_1$  and  $\Psi_2$ . The linear stage ends when the minimum in each period reaches some level  $\Psi_1'$  below which no energy is gained in decreasing  $\Psi$  further. Determination of the exact value of  $\Psi_1'$  is a difficult task and it should be system dependent, but its location must be above  $\Psi_1$  and in the convex part of the coarse grained free energy,  $F(\Psi)$ , curve at temperature  $T$ . The latter is also schematically drawn on the right hand side of Fig. 1-a.

In a second stage, the system is still decreasing its energy within each period  $\lambda_*$  by increasing  $\Psi$  in the high- $\Psi$  part of the motif (hill) while expanding laterally the flat region at  $\Psi_1'$  (plain). The periodic profile  $\Psi(r)$  loses its symmetry with respect to the  $\Psi_0$  level. The new pattern is drawn on Fig. 1-b. The development of flat regions results in the rise of higher order harmonics in the roughness

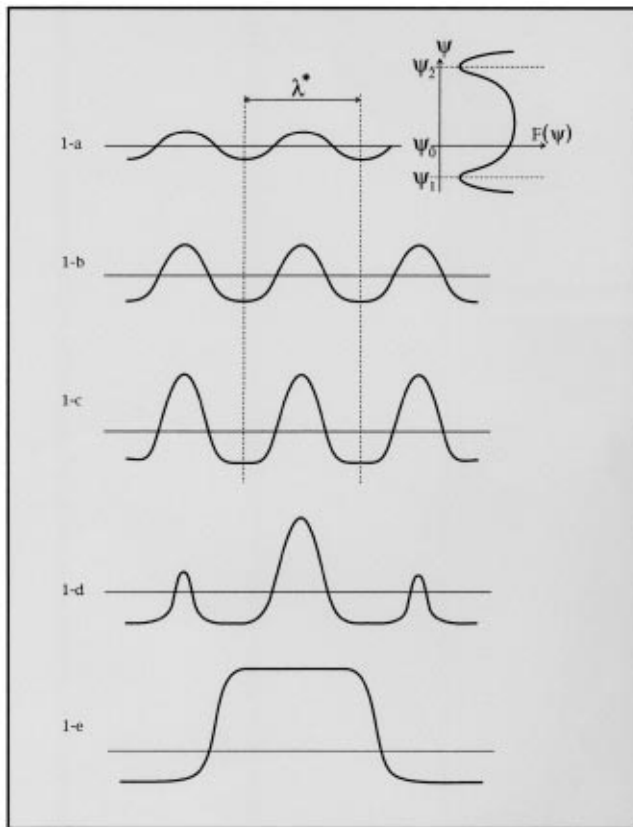


FIG. 1. Theoretical evolution of the order parameter profile during the spinodal decomposition kinetics.

spectrum. This is the first nonlinear effect. The second stage ends when the energetic price for a further increase of the slope  $|\nabla\Psi|$  becomes too high [6]. This situation is illustrated in Fig. 1-c. Up to that point, the pattern evolution has been governed by local exchanges of neighboring  $(d + 1)$ -volume elements. Given a specific  $F(\Psi, T)$  diagram and a specific dissipation rule, it can be described by local hydrodynamics in a finite volume  $\Psi_0\lambda_*^d$  of the  $\{r, \Psi\}$  space. Had the system been of size  $\lambda_*^d$ , its evolution would have been exactly the same, and would have been completed at the end of the second stage. One period in Fig. 1-c is actually an equilibrium pattern for this finite system. Hills in it are essentially made of what would be unstable matter in a larger system; they can be viewed as quasistable pieces of interfacial matter. In each domain  $\lambda_*^d$ , the chemical potential  $\mu(\Psi_0, \lambda_*)$  is uniform.

The third stage is a slower exchange of  $(d + 1)$  volumes of matter between neighboring periods. It implies long range transport of  $\Psi$  and loss of the conservation constraint at the scale  $\lambda_*$ . The driving force is the difference in chemical potential between adjacent periods. Note that even the simplified monomodal pattern of Fig. 1-c is unstable. We shall return to that point at the end of this section. Since the kinetics is now governed by long range exchanges, while the evolution of the profile  $\Psi(r)$  is governed by faster short range material transport, the shape

of the latter remains an equilibrium one. The third stage is therefore a ripening process involving  $\lambda_*$  units permanently equilibrated. It is illustrated in Fig. 1-d. Larger hills grow at the expense of smaller ones. The roughness spectrum enriches with additional wavelengths, generated by the disappearance of small hills on the spot. They are thus integer multiples of  $\lambda_*$ . Several iterations can be necessary for the surviving hills to reach  $\Psi_2$ ;  $\Psi_1'$  at each step becomes closer and closer to  $\Psi_1$ . It constitutes a cascade mechanism similar to those encountered in non-linear dissipative phenomena such as turbulence decay [7]. The third stage ends with the formation of domains of the minority phase, as shown in Fig. 1-e. They will evolve afterwards according to the classical late stage ripening models [8], with the line tension as a driving force.

Three remarks will close this section. The first concerns the beginning of the second stage: Real systems do not reduce to a single mode model, so that random flat regions are expected to develop instead of the regular pattern of Fig. 1-b; they can be considered as isolated drops of the majority phase or “antiphase” domains [9]. They rapidly multiply, and, if  $d \geq 2$ , they percolate and encircle isolated hills which are drops of interfacial matter. The second remark concerns the situation of Fig. 1-c: The height of the characteristic bevel blocked hills remains below the  $\Psi_2$  level because we assume that a period  $\lambda_*^d$  does not contain enough  $(d + 1)$  material for a full domain at  $\Psi_2$  to develop. This statement is not necessarily true for every system at every unstable composition  $\Psi_0$ . Let us therefore keep in mind that one cannot always reach the “bevel early hills.” The third remark concerns the third stage: The characteristic length for efficient material exchange has now jumped from molecular to  $\lambda_*$  level, so that the pertinent driving potential for the kinetics is  $\mu(\langle\Psi\rangle)$ , where the average  $\langle\Psi\rangle$  is taken over a domain  $\lambda_*^d$ . In the monomodal model, the third stage starts with a uniform distribution of joint blocks  $\lambda_*^d$  at  $\Psi_0$ , which is unstable. The third stage can thus be treated as a spinodal decomposition of the system of  $\lambda_*^d$  blocks, e.g., as a rescaled initial stage, and therefore linear. The same idea is transposable to the next step in the cascade. This rescaling procedure is close in spirit to the line followed in the phenomenological theory of Furukawa [10].

Experiments were carried out on thin films of a symmetric polystyrene-polybutylmethacrylate diblock copolymer with a molecular weight  $M_n = 82000$  g/mol and a polydispersity index  $I_p = 1.04$ , deposited on a solid substrate. It was synthesized by anionic polymerization. In the ordered state [11] the film is made everywhere of an integer number of bilayers (3 or 4), each with a thickness  $L = 300$  Å. The starting disordered state is a homogeneous solid film with a thickness  $h_0 = 3,4L$  (sample 1) or  $h_0 = 3,6L$  (sample 2). In the final state, the two thicknesses  $h_1 = 3L$  and  $h_2 = 4L$  are coexisting along the surface, forming islands (sample 1) or holes

(sample 2). The quench is obtained by annealing the sample at  $T = 150^\circ\text{C}$ , where the copolymer exhibits a smectic ordering with homeotropic anchoring. The difference in free surface tensions between the two components is large enough to avoid the formation of the metastable states described in Ref. [12]. The order parameter of the transition is defined as  $\Psi = [2h(x,y) - 7L]/L$ , where  $h(x,y)$  is the local thickness at position  $(x,y)$  on the surface. The geometrical vocabulary of part one thus makes direct sense for this system, in which  $d = 2$ .

Figure 2 presents four typical steps in the experimental kinetics of each sample. Each step is illustrated by three representations directly delivered by the atomic force microscope: The image is a top view of the copolymer film; the bottom curve is a section taken along the dark line on the image; the curve on the right hand side is a histogram of the image, which is, in our case, the distribution  $d\Sigma/d\Psi$  of the order parameter along the surface,  $d\Sigma$  being the sample area covered by  $[\Psi, \Psi + d\Psi]$ .

Let us first focus our attention on the islands kinetics (right column) which is a concrete realization of the general scheme discussed in the first section. The first

step corresponds to Fig. 1-a. It exhibits a surface roughness with a root mean square roughness of  $10 \text{ \AA}$  over a  $20 \mu\text{m} \times 20 \mu\text{m}$  area to be compared with the initial value of  $5 \text{ \AA}$ . The height distribution is symmetric with respect to its average value  $h_0$ , and the roughness spectrum, which is not monomodal, has a dominant period of  $0.75 \mu\text{m}$ . This roughness is continuously and rapidly increasing from the beginning of the kinetics. We take this instability as a signature of a spinodal decomposition.

The second step corresponds to 1-c. Flat regions are coexisting with transient hills of height smaller than  $L$ . The histogram, highly nonsymmetric, is made of one strong peak coexisting with a long tail extending towards, but not up to,  $h_2$ . Note that the distinction between stages 1-b and 1-c is not easy to make in practice because the roughness spectrum is not monomodal. However, stage 1-b is expected to be so fast that step 2 in Fig. 2 must probably correspond to stage 1-c. The third step corresponds to the stage where some islands finally reach the  $\Psi_2$  level. A second peak is just appearing in the distribution, and a maximum height, common to many islands, becomes visible in the section. It corresponds to the end of the cascade mechanism described in the first section, say, somewhere in between illustrations 1-d and 1-e. Note that the surface coverage by islands is increasing and therefore  $\Psi_1'$  is decreasing between the second and the third step. The fourth step at last corresponds to Fig. 1-e. Islands with a height  $L$  are well formed and start growing in diameter according to the usual ripening mechanism [8]. The height distribution exhibits two well defined narrow peaks. Focusing now exclusively on the histograms of Fig. 2, please note the qualitative resemblance between the actual series of shapes observed as time goes, and the theoretical evolution that was numerically predicted by Langer, Bar-on, and Miller for strongly off-critical quenches in Ref. [13].

Figure 3 presents a zoom in space and time of the sample in stage 1-c. It shows successive perspective views of the same  $9 \times 9 \mu\text{m}^2$  portion of the surface sample for annealing times 290, 530, 790, and 1460 sec, which approximately covers the time range from the second to the third line of images in Fig. 2, right hand column. Figure 3 gives strong support to the subharmonic nonlinear mechanism proposed in the general part for stage 1-c: Large transient islands are growing on the spot to the expense of small transient islands disappearing on the spot. Moreover, the shape of the growing islands is slowly evolving, in conformity with their description as quasiequilibrium structures.

To summarize, the islands formation closely resembles the general scheme given in the first section. However, the interpretation of this ordering process in terms of two-dimensional phase transition kinetics is not universally accepted. The major argument against it is the following: The evolution of the surface topography is just a consequence of bulk ordering in the film; it is known to

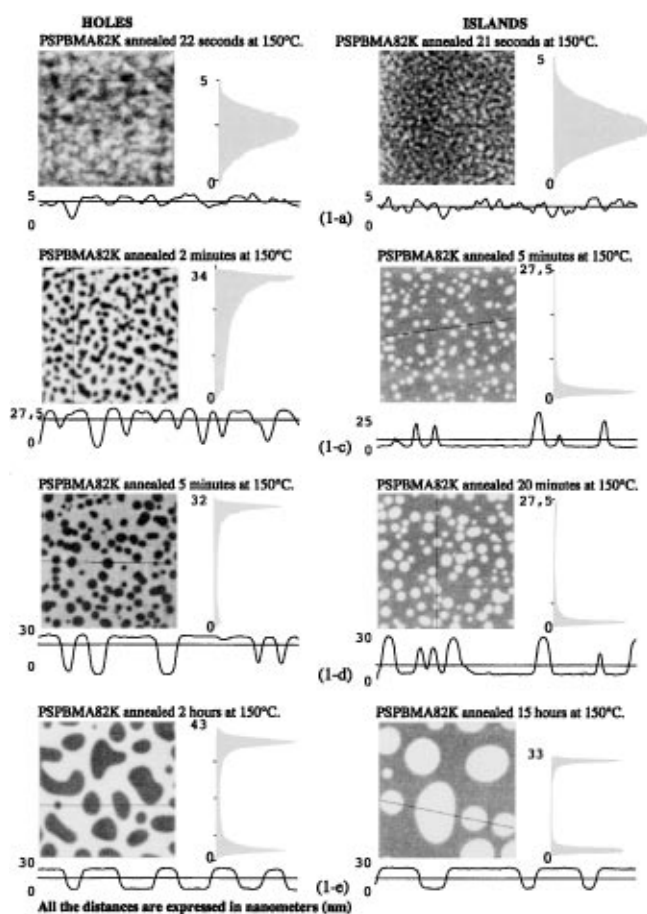


FIG. 2. Evolution of the free surface of a thin film of symmetric diblock copolymers with the annealing time at  $150^\circ\text{C}$  under vacuum: Top view (upper left), section (bottom), and height histogram (upper right).

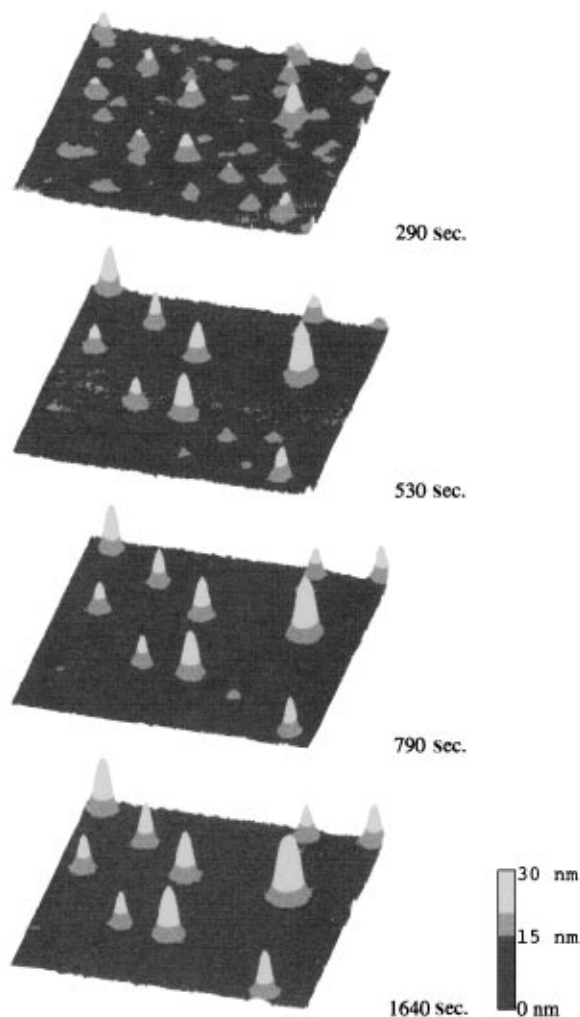


FIG. 3. Evolution with annealing time, of the same portion ( $9.22 \mu\text{m} \times 9.22 \mu\text{m}$ ) of the free surface of sample 1 at  $150^\circ\text{C}$ : experimental evidence of the subharmonic nonlinear mechanism.

start from the solid and progressively extend towards the free surface [14]. Therefore the appearance of flat regions in the early stage results from the fact that  $h_1$  is smaller than  $h_2$  and has nothing to do with the behavior of the majority phase in a 2D phase transition kinetics.

Our answer against this argument is experimental. It is given in the left column of Fig. 2, which illustrates a kinetics similar to that of the right column for the formation of holes. Every step is transposable from one column to the other. Differences are only quantitative; they concern the exact shapes of the order parameter profiles, the time intervals between corresponding steps, the time evolution of the surface fraction covered by the majority phase, and so on. All qualitative features

are conserved. In particular, the second image from the top demonstrates the existence of flat regions at  $h_2$ , coexisting with a wide distribution of thicknesses spreading towards, but not down to,  $h_1$ . Hence, the argument above is contradicted by this experiment. Early flat regions correspond, in both cases, to the majority phase.

To conclude, we have given a description of the spinodal decomposition in direct space. It contrasts with the formidable amount of work done in the reciprocal Fourier space and hopefully brings a new and more intuitive understanding of the mechanism. It also brings new concepts such as the existence of the blocked hills or the succession of two different nonlinear stages (harmonic and subharmonic) in the so-called intermediate regime and also new technical solutions like the possibility of treating blocked hills as equilibrium structures or a way to linearize the second nonlinear stage. A similar study is under progress on nucleation kinetics.

We thank Rashmi Desai and David Andelman for helpful discussions, and J.P. Lingelser for his valuable assistance in the synthesis of the copolymer sample.

\*Permanent address: Laboratoire Léon Brillouin (CEA CNRS), 91191 Gif sur Yvette Cedex, France.

†To whom correspondence should be sent.

- [1] J.D. Gunton, M. San Miguel, and P.S. Sahni, in *Phase Transitions and Critical Phenomena*, edited by C. Domb and J.L. Lebowitz (Academic Press, London, 1983), Vol. 8.
- [2] P. Guenoun, F. Perrot, and D. Beysens, *Phys. Rev. Lett.* **63**, 1152 (1989).
- [3] M. Seul, N.Y. Morgan, and C. Sire, *Phys. Rev. Lett.* **73**, 2284 (1994).
- [4] J.S. Langer, in *Proceedings of the 1989 Beg Rohu School*, edited by C. Godreche (Cambridge University Press, Cambridge, England, 1992), pp. 297–363.
- [5] M. Hillert, *Acta Metall.* **9**, 525 (1961).
- [6] J.W. Cahn and J.E. Hilliard, *J. Chem. Phys.* **28**, 258 (1958).
- [7] C. Sire, *Bull. Sté Française Phys.* **101**, 24 (1995).
- [8] I.M. Lifshitz and V.V. Slyozov, *J. Phys. Chem. Solids* **19**, 35 (1961).
- [9] D. Katzen and S. Reich, *Europhys. Lett.* **21**, 55 (1993).
- [10] H. Furukawa, *Phys. Rev. A* **23**, 1535 (1981).
- [11] B. Collin, D. Chatenay, G. Coulon, D. Ausserré, and Y. Gallot, *Macromolecules* **25**, 1621 (1992).
- [12] M. Maaloum, D. Ausserré, D. Chatenay, and Y. Gallot, *Phys. Rev. Lett.* **70**, 2577 (1993).
- [13] J.S. Langer, M. Bar-on, and H.D. Miller, *Phys. Rev. A* **11**, 1417 (1975).
- [14] T.P. Russell, G. Coulon, V.R. Delin, and D.C. Miller, *Macromolecules* **22**, 4600 (1989).